JCTC Journal of Chemical Theory and Computation

pubs.acs.org/JCTC Article

Predicting Ligand-Dissociation Energies of 3d Coordination Complexes with Auxiliary-Field Quantum Monte Carlo

Benjamin Rudshteyn,[⊥] Dilek Coskun,[⊥] John L. Weber, Evan J. Arthur, Shiwei Zhang, David R. Reichman, Richard A. Friesner, and James Shee*

Cite This: *J. Chem. Theory Comput.* 2020, 16, 3041−3054 Read Online

ACCESS | Metrics & More | Article Recommendations | Supporting Information

ABSTRACT: Transition-metal complexes are ubiquitous in biology and chemical catalysis, yet they remain difficult to accurately describe with *ab initio* methods because of the presence of a large degree of dynamic electron correlation, and, in some cases, strong static correlation which results from a manifold of low-lying states. Progress has been hindered by a scarcity of high-quality gas-phase experimental data, while exact *ab initio* predictions are usually computationally unaffordable because of the large size of the relevant complexes. In this work, we present a data set of 34 tetrahedral, square planar, and octahedral 3d metal-containing complexes with gas-phase ligand-dissociation energies that have reported uncertainties of ≤2 kcal/mol. We perform all-electron phaseless auxiliary-field quantum Monte Carlo (ph-AFQMC) calculations utilizing multi-determinant trial wave functions selected by a black box procedure. We compare the results with those from the density functional theory (DFT) with the B3LYP, B97, M06, PBE0, ωB97X-V, and DSD-PBEP86/2013 functionals and a localized orbital variant of the coupled cluster theory with single, double, and perturbative triple excitations (DLPNO-CCSD(T)). We find mean averaged errors of 1.07 ± 0.27 kcal/mol for our most sophisticated ph-AFQMC approach versus 2.81 kcal/mol for DLPNO-CCSD(T) and 1.49−3.78 kcal/mol for DFT. We find maximum errors of 2.96 ± 1.71 kcal/mol for our best ph-AFQMC method versus 9.15 kcal/mol for DLPNO-CCSD(T) and 5.98−13.69 kcal/mol for DFT. The reasonable performance of a number of DFT functionals is in stark contrast to the much poorer accuracy previously demonstrated for diatomic species, suggesting a moderation in electron correlation because of ligand coordination in most cases. However, the unpredictably large errors for a small subset of cases with both DFT and DLPNO-CCSD(T) methods leave cause for concern, especially in light of the unreliability of common multireference indicators. In contrast, the robust and, in principle, systematically improvable results of ph-AFQMC for these realistic complexes establish the method as a useful tool for elucidating the electronic structure of transition-metal-containing complexes and predicting their gas-phase properties.

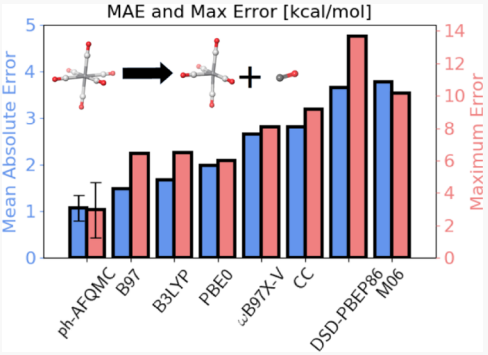

INTRODUCTION

The unique electronic structure of transition metals enables a rich variety of chemical reactivity, harnessed in systems ranging from those found in the fields of chemical catalysis,[1] biology,[2] and materials science.[3] The presence of multiple quantum states within an accessible energy range allows for reaction mechanisms involving sequential redox events and subtle transformations between spin-states, for example, in clusters of Mn atoms in Photosystem II (PSII) or Fe and Mo atoms in nitrogenases.[4−7] Furthermore, the coordination of small molecules to single metal ions is an important motif in drug design,[8] and the correlations exhibited in the copper oxide layers of cuprate materials play a central role in the phenomenon of high-temperature superconductivity.[9,10]

Ab initio modeling has the potential to yield essential insights into these transition-metal systems. However, exact methods scale exponentially with the system size and are thus only applicable to small molecules. Many groups have used the density functional theory (DFT) to examine the electronic structure and reaction mechanisms of coordinated transition-metal complexes, including the active sites of PSII[6,7] and cytochrome P450,[11,12] catalysts for water oxidation,[13] CO_2 reduction,[14] and sensitizers for optical upconversion.[15] However, there are a number of uncertainties which may cast doubt upon their conclusions, chief among them possible errors because of unphysical electron delocalization and strong correlation. Furthermore, as the majority of parameterized density functionals (DFs) and dielectric continuum solvation models have been trained on organic compounds (e.g., the ωB97X-V[16] and ωB97M-V[17] functionals and the SMD solvation model[18]), it is reasonable to suspect the accuracy

Received: January 20, 2020
Published: April 15, 2020

https://dx.doi.org/10.1021/acs.jctc.0c00070
J. Chem. Theory Comput. 2020, 16, 3041−3054

of the resulting predictions in the domain of transition-metal chemistry.

The pronounced lack of reliable and precise gas-phase experimental data for realistic transition-metal systems, as illustrated by recent theoretical benchmarking studies, exacerbates these issues.[19−29] This scarcity of experimental measurements is in stark contrast to the large amount of reliable experimental values for organic molecules, which has enabled very accurate parameterizations of DFT functionals and a thorough validation of methods such as CCSD(T), which can readily achieve ∼1 kcal/mol accuracy for typical organic molecules.[30]

The accuracy of CC methods, most frequently CCSD(T), is often assumed to carry over to transition-metal systems, as evidenced by a number of studies that have attempted to draw conclusions about the accuracy of DFT by comparing against reference CC values.[31−35]

However, the reliability of CC methods for transition-metal systems, even when multireference effects are approximated, has been the subject of vigorous debate, as illustrated by recent studies on transition-metal diatomic ligand systems.[24,36−41] de Oliveira-Filho and co-workers found that even multireference CCSD(T) could not predict the bond dissociation energies (BDEs) for some diatomics accurately with respect to experimental measurements. A recent study by Head-Gordon and co-workers found that high levels of CC, up to CCSDTQ, are required for chemical accuracy against an exact method known as adaptive sampling configuration interaction results, albeit in a small basis set.[42] Wilson and co-workers collected a set of 225 heats of formation for compounds with first row transition-metal atoms.[24] They found good performance for their composite CC scheme versus a subset of experimental data with small uncertainties, but the mean absolute error (MAE) of around 3 kcal/mol may be insufficient for many chemical applications. Reiher and co-workers considered transition-metal ligand-dissociation energies of very large molecules and showed that a localized variant of CCSD(T) utilizing domain—based pair natural orbitals (DLPNO-CCSD(T))[43,44] resulted in pronounced errors, for example, ∼9.3 kcal/mol for the cleavage of a Cu complex.[45]

An alternative benchmarking approach involves filtering out strongly correlated cases with multireference diagnostics and benchmarking DFT against CC methods only for the single-reference subset of molecules. Hansen, Checinski, and co-workers developed the MOR41 test set of organometallic reactions of medium−large size.[34] They removed open-shell, multireference cases (with, e.g., FOD and T1 diagnostics). Recently, the properties of a set of transition-metal atoms and oxide diatomics, in which strong multireference cases were removed, have been predicted by a large number of *ab initio* methods.[41] In our view, this strategy is less than ideal not only because a large subset of relevant chemistry is excluded, but, moreover, because the utility of affordable multireference indicators has increasingly been called into question. Indeed, studies have found mixed success for different kinds of multireference diagnostics,[36−39,46] making it hard to judge a priori when single-reference methods would be appropriate.

In this work, we assemble a test set of gas-phase ligand dissociation measurements with low reported experimental uncertainties. On this set, we use auxiliary-field quantum Monte Carlo with the phaseless constraint (ph-AFQMC),[47,48] accelerated by a correlated sampling technique[49] and our implementation on graphical processing units.[50] We have shown that this method yields robust accuracy for the ionization energy of transition-metal atoms (MAE = 0.5 ± 0.2 kcal/mol)[50] and the dissociation energy of transition metal-containing diatomics (MAE = 1.4 ± 0.4 kcal/mol), similar to the diatomic sets discussed above.[40] The present study marks a large step forward, to more relevant transition metal-containing systems. We demonstrate that ph-AFQMC with correlated sampling yields accurate BDE predictions for various tetrahedral, square planar, and octahedral complexes containing first row transition-metal atoms and ligands including dihydrogen, chloride, dinitrogen, aqua, ammonia, carbonyl, and formaldehyde. We, then, validate the performance of a representative set of DFT functionals and the DLPNO-CCSD(T) method. Consistent with our expectation, we find that single-reference methods such as DFT and the CC hierarchy perform better for coordinated metal compounds compared to the case of diatomic dissociation (as ligand coordination can lower the degree of degeneracy of the metal atomic d orbitals, and the bonds have less covalent than ionic character). However, we demonstrate that ph-AFQMC still produces a significant improvement in terms of MAE and maximum error (MaxE). The large MaxEs in our study for single-reference methods suggest that, for a number of these transition-metal coordination compounds, accurate prediction of the BDE is not as simple as the ligand−metal dative bonding picture might suggest, requiring computational approaches capable of handling strong correlation.

Our results show that ph-AFQMC can consistently produce benchmark-quality results, and with a computational cost which scales as a low polynomial with the system size (excluding the cost of obtaining "the complete active space self-consistent field (CASSCF)" trial wave functions). A unique advantage of the ph-AFQMC methodology is that the accuracy of its predictions can be systematically improved by utilizing trial wave functions of increasing quality. Therefore, an additional aim of this work is to establish a computational protocol which can achieve robust accuracy at a minimal computational cost and which can scale to larger systems, exhibiting the same chemical motifs. Our results suggest a protocol which involves ph-AFQMC calculations with truncated CASSCF trial wave functions of $O(100)$ determinants (ph-AFQMC/CAS) in the triple-zeta basis, extrapolated to the complete basis set (CBS) limit with ph-AFQMC with unrestricted Hartree Fock (UHF) calculations in the triple- and quadruple-zeta basis sets. This method will extend accurate reference datasets for future benchmarking studies of approximate methods such as DFT and accurate classical potentials for transition-metal ions. In addition, the level of accuracy of the widely employed quantum-chemical methods included in this study provides a sense of the accuracy to be expected for calculations on similar four- and six-coordinated 3d metal complexes that are ubiquitous in fields such as biology and catalysis.

SELECTION OF EXPERIMENTAL DATA

We selected gas-phase experimental BDE data with less than or equal to 2.0 kcal/mol uncertainty from the recommended values in the handbook compiled by Luo.[51] Most of the measurements can also be found in the work by Rodgers and Armentrout.[52] For $TiCl_4$[53] and $[Ni(H_2O)_6]^{2+}$,[54] more recent experimental measurements have been used. The average uncertainty for the molecules included in the present test set is 1.05 kcal/mol. Most of the measurements were performed with

https://dx.doi.org/10.1021/acs.jctc.0c00070
J. Chem. Theory Comput. 2020, 16, 3041−3054

the threshold collision-induced dissociation (TCID) technique except for $TiCl_4$,[53] $CrCO_5H_2$,[55] and $[V(H_2O)(H_2)_3]^+$,[56] which were measured with effusion beam mass spectroscopy, transient infrared spectroscopy for kinetic analysis, and temperature-dependent equilibrium, respectively. The latter technique was used for all other H_2 complexes as well. We also compare the recommended values to several alternatives provided by Rodgers and Armentrout.[52]

The selected compounds are depicted schematically in Figure 1. These experimental data are mostly extrapolated to 0 K and can therefore be directly compared with quantum chemical calculations. The two exceptions are $TiCl_4$ and $CrCO_5H_2$, which are measured at 298 K. All the metal complexes have +1 net charge, except for $[Ni(H_2O)_6]^{2+}$, $TiCl_4$, and $CrCO_5H_2$. The full list of reactions, including the multiplicities of the participating species, is given in the Supporting Information.

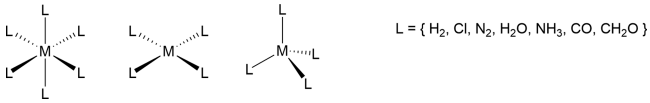

Figure 1. Types of transition-metal compounds studied. M can be any 3d transition metal from Ti to Cu.

COMPUTATIONAL DETAILS

The geometries, reorganization energies (vide infra), and enthalpic corrections [just the zero-point energy (ZPE) for cases where the 0 K extrapolated experiment is available, as discussed above] were obtained with DFT calculations with the B3LYP functional[57−59] and cc-pVTZ-dkh[60−63] basis set using the ORCA program package.[64] The frequencies were unscaled, as scaling factors close to 1 would hardly change the difference in ZPE's of reactant and products compared to the uncertainty of the experiments. Details regarding occasional small imaginary frequencies and integration grids are given in Section IV of the Supporting Information. The B3LYP geometries and ZPEs are utilized in all of the methods in our study, including the ph-AFQMC method. Using a single method to calculate geometries and frequencies ensures that any biases because of these are uniformly applied to all methods.

The unrestricted or U DLPNO-CCSD(T) calculations were also done with ORCA using "TightPNO" (strict energy cutoff criteria for correlation between localized orbitals) localization parameters and the cc-pV*x*Z-dkh basis sets, x = T, Q, and are extrapolated to the CBS limit using the procedure built into ORCA,[64] as discussed in the Supporting Information. We used the corresponding cc-pV*x*Z\C auxiliary basis sets for the DLPNO calculations. Because for DLPNO-CCSD(T) and for ph-AFQMC, as discussed below, we extrapolate our results to the CBS limit, we believe that the error from the lack of inclusion of diffuse functions should be small, especially as none of the species we study is anionic. That said, our study does have lone pairs, the treatment of which may benefit slightly from the use of diffuse functions.[65] Our calculations utilize the "semicanonical" or "T_0" approximation in the perturbative triples correction, which has been found to be adequate in many cases.[66] A recent study involving transition-metal complexes found that use of the T_0 method can lead to differences from full CCSD(T) of around 4 kcal/mol.[67] We have compared the T_0 and "T_1" (which more closely approximates the triples perturbation[43]) methods on the BDEs of $[Ni(H_2)_4]^+$ and $[Ni(H_2O)_4]^+$ and found similar results within 0.5 kcal/mol. In light also of the relative computational expedience of the former method, we utilize the T_0 approach throughout this work.

We found similar results from the restricted open-shell (R) version of DLPNO-CCSD(T). For example, the BDE of $[V(CO)_6]^+$, which exhibits ∼20% spin contamination, is 26.6 kcal/mol with U as opposed to 26.7 kcal/mol with R. Nevertheless for the vast majority of molecules, the spin contamination was found to be much less than 15−20%, thus we used the U approach as it affords a better description of strong correlation, in the event it is encountered. We also found that, except for the dihydrogen complexes, running full CCSD(T) would be prohibitively expensive, particularly in the QZ basis set. Because we want to use the same CC method on all the complexes, we decided to employ the DLPNO approximation. We have run full CCSD(T) on the BDE of $[Ni(H_2)_4]^+$ as a test case and found the same BDE at TZ and QZ, and at the CBS limit to within 1 kcal/mol. We also used the "NoFrozenCore" keyword in ORCA indicating that we correlated all electrons, although the DLPNO approach, as implemented, will not typically correlate core−valence electron pairs based on energetic thresholds. Regardless, we tested freezing the core electrons for $[Ni(H_2O)_4]^+$ and found that the BDE decreased by about 0.5 kcal/mol at the TZ, QZ, and CBS levels, which is fairly small. The DKH2 relativistic correction was used for all DFT and CC calculations.[68]

Integrals for ph-AFQMC were obtained with PySCF.[69] The exact two-component (x2c) relativistic Hamiltonian[70] was used in place of DKH2. As in our previous work,[40,49,50,71] the imaginary time step for the ph-AFQMC propagation, utilizing single precision floating point arithmetic, was 0.005 E_h^{-1}. The walker orthonormalization, population control, and local energy measurements occurred every 2, 20, and 20 steps, respectively. We utilized a modified Cholesky decomposition of the electron repulsion integrals with a cutoff of 10^{-5}. Walkers were initialized with the RHF/ROHF determinant.

The correlated sampling approach[49] can converge energy differences between similar states by employing a shared set of auxiliary fields for a short projection time, providing accurate results with smaller statistical errors versus uncorrelated ph-AFQMC (the latter would need to run longer projections to reach the same statistical accuracy). This approach performs most efficiently when the ligand being removed is small, particularly a hydrogen atom, as indicated by our previous work, in which the reduction in statistical error versus the uncorrelated approach was several times larger for MnH than for MnCl.[40] Similar behavior is found for the transition-metal complex systems studied here, as shown in Figure 2 for $[Cu(H_2)_4]^+$. In fact, correlated sampling may work better for these complexes than it did for the diatomics because ≪50% of the system is being changed. Finally, we note that correlated sampling also can improve the accuracy of the predicted results in certain situations.[40,50]

In the context of computing BDEs, our ph-AFQMC calculations used correlated sampling for the difference in energy between the original coordination compound (M−L) and the species missing a ligand (M), that is, the same geometry but with ghost basis functions centered around the positions of the missing nuclei that comprise the ligand. If the difference in energies was not converged before 15 E_h^{-1}, uncorrelated, separate ph-AFQMC calculations are performed

https://dx.doi.org/10.1021/acs.jctc.0c00070
J. Chem. Theory Comput. 2020, 16, 3041−3054

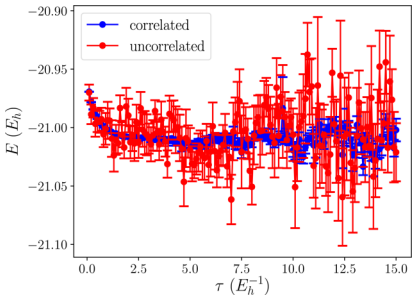

Figure 2. Correlated sampling ph-AFQMC calculations using Summit GPUs; statistical errors from correlated and uncorrelated sampling approaches are compared for the Cu−H_2 BDE of the $[Cu(H_2)_4]^+$ molecule.

for the optimized structures of both states without ghost basis functions, using a population control scheme in which walkers with large weights are duplicated while those with small weights are randomly destroyed for the optimized structures of both states without ghost basis functions.[72] The isolated ligand (L) was also treated with the population control approach.

The BDE, as computed by ph-AFQMC with correlated sampling, is given as follows

$$\mathrm{BDE} = (H(\mathrm{M}) - H(\mathrm{M-L})) + H(\mathrm{L}) - \lambda \quad (1)$$

where H is the enthalpy including the zero-point corrections and the nuclear repulsion energy. The reorganization energy, λ, is defined as the difference in energy between the product (complex with the ligand dissociated) in its optimal geometry and in the reactant geometry, optimized with the ligand, but with the ligand atoms deleted. λ is computed via B3LYP/cc-pVTZ-dkh (the same methods described above). We optimize and compute the energy of L separately, which effectively takes into account ligand reorganization. The calculation of BDEs is illustrated in Figure 3.

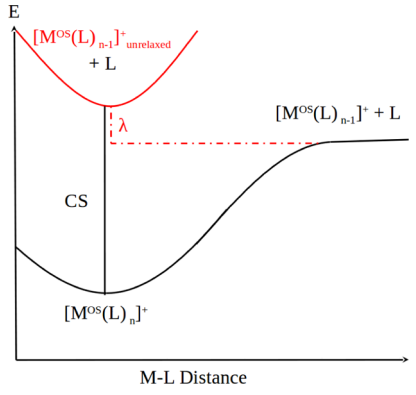

Figure 3. Schematic of BDE calculations performed in this work. OS abbreviates the oxidation state and CS indicates the energy measured by the correlated sampling approach.

To give a sense of the required computational cost, a correlated sampling ph-AFQMC calculation for $[Fe(N_2)_4]^+$ took about 267 node hours on Summit, using a truncated CASSCF trial wave function containing 1195 determinants. This reflects the use of 20 repeats (i.e., independent trajectories with different random number seeds), each using 20 nodes with 6 GPUs each (each repeat ran for about 42 min).

The CBS limit for the ph-AFQMC calculations was estimated by extrapolation using DLPNO-CCSD(T) values with the cc-pVxZ-dkh basis sets, x = T, Q, using exponential and $1/x^3$ forms for the mean field (i.e., UHF) and correlation energies, respectively, as in our previous work.[40] If the ph-AFQMC correlation energy with cc-pVTZ-dkh is significantly different from DLPNO-CCSD(T), or if comparison of the extrapolated value with experiment indicates a potential problem (our target accuracy is <3 kcal/mol, which has been referred to as "transition-metal chemical accuracy"[73]), then full extrapolation within ph-AFQMC is performed utilizing both cc-pVTZ-dkh and cc-pVQZ-dkh basis sets (for dihydrogen or chloro compounds). In some cases, we instead extrapolate with a UHF trial-based ph-AFQMC procedure, which seems to be a good compromise between speed and accuracy. See Tables S4 and S5 for details and Section V in the Supporting Information for an overview of how extrapolation is done. A summary of the typical ph-AFQMC calculation workflow is provided in Section VIII of the Supporting Information. The standard for selecting which CBS extrapolation method to use is usually the scaling factor mentioned above but otherwise is taken to be agreement with experiment to within 3 kcal/mol.

Apart from the basis set extrapolations, the ph-AFQMC calculations utilized CASSCF trial wave functions. The size of the CASSCF trial wave function for the metal-containing species was automatically selected via the atomic valence active space (AVAS) procedure where only those B3LYP ROKS orbitals that overlap significantly with the 3d and/or 4d atomic orbitals (from the minimal atomic basis set called "MINAO" as used by Knizia[74] or from the atomic natural orbital (ANO-RCC) basis set) of the metal were included (as noted in the Supporting Information in Table S3).[75] The single numerical overlap threshold parameter was used to generate sequentially larger active spaces to determine what active space size is needed to reach chemical accuracy. The active space for the ligand was selected by either using the valence set of electrons and orbitals or using a large number for electrons and orbitals to ensure convergence. Typically >98% of the weight of the CI coefficients was retained. The active spaces were selected so that the active space for the reactant and product metal species was similar (either the same or off by one orbital and two electrons), which often requires the same AVAS threshold.

ph-AFQMC uncertainties reflect the standard error, as obtained from averaging the energy values after the equilibration time along trajectories obtained from propagation in imaginary time. Then, the uncertainty of a ph-AFQMC BDE is calculated by quadrature (taking the square root of the sum of the squares) from the uncertainties of the individual ph-AFQMC calculations (one for every species in the reaction). When comparing to the experiment, the experimental uncertainty is incorporated via quadrature as well.

We compare ph-AFQMC with the B3LYP, M06,[76] and PBE0[77] functionals because they are arguably the most popular and B97 because this functional performed the best in our previous study.[40] To explore the performance of range-correction and the nonlocal correlation approach, we include the ωB97X-V functional.[16] We also consider the double hybrid functional, DSD-PBEP86. It is available in ORCA and has been shown to perform very well,[78−81] accelerated by the resolution of identity approximation on the MP2 part. In this study, we used the "DSD-PBEP86/2013" functional, which has slightly different parameters than DSD-PBEP86, but refer to it as DSD-PBEP86 throughout the paper.

https://dx.doi.org/10.1021/acs.jctc.0c00070
J. Chem. Theory Comput. 2020, 16, 3041−3054

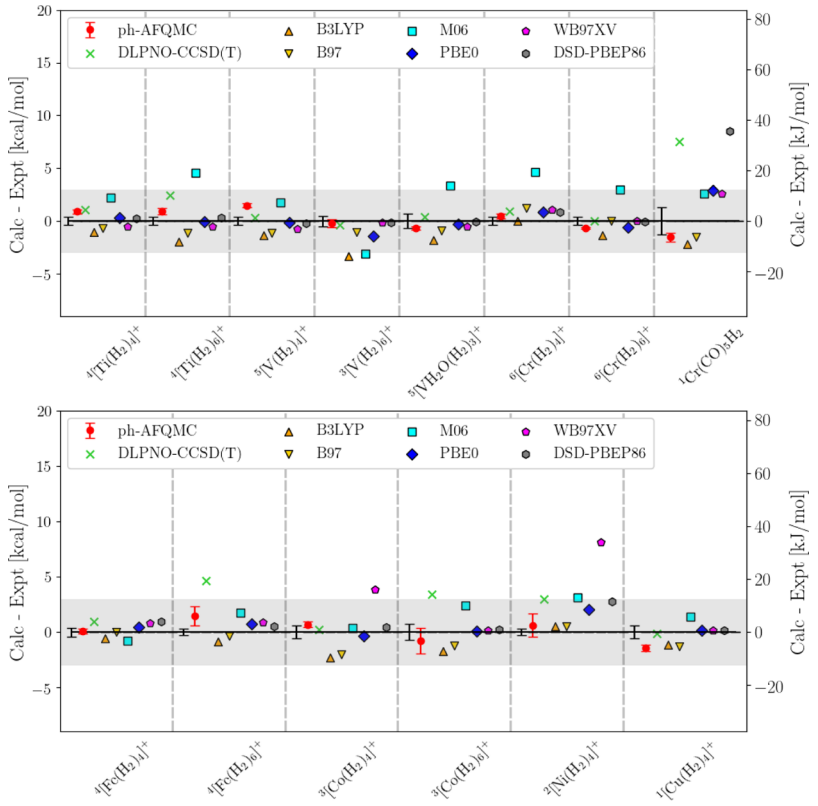

Figure 4. Deviations [kcal/mol on the left and kJ/mol on the right] of computational methods for the dihydrogen set of bond dissociation reactions where the H_2 that leaves are given at the end of the formula. The multiplicities in the superscript at the start of the molecular formula apply for both reactant and dissociated product, except for $^5[V(H_2)_5]^+$. The gray band indicates ±3 kcal/mol [12.5 kJ/mol] accuracy.

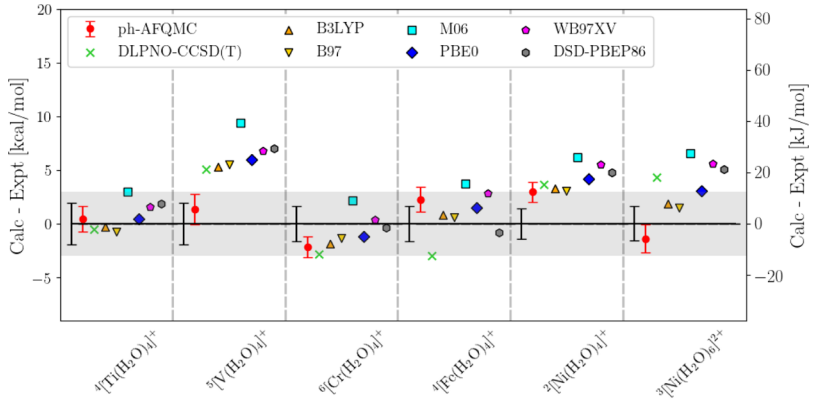

Figure 5. Deviations [kcal/mol on the left and kJ/mol on the right] of computational methods for the aqua set of bond dissociation reactions. The multiplicities in the superscript at the start of the molecular formula apply for both reactant and dissociated product. The gray band indicates ±3 kcal/mol [12.5 kJ/mol] accuracy.

Because analytical gradients have not yet been implemented in ORCA for all of the functionals in this study, we decided to use B3LYP optimized geometries and performed single-point energy calculations. Grid and density-initialization choices are described in Section IV of the Supporting Information.

For all DFT and HF [the latter is used as a reference wave function for DLPNO-CCSD(T)] calculations, we found it essential to perform a stability analysis to ensure that the lowest energy SCF solution was obtained.

RESULTS AND DISCUSSION

The deviations of the computed BDEs from experiment are presented in Figures 4−8. Values of the BDEs are given explicitly in Tables S1 and S6. Tables 1 through 6 show statistical metrics including mean signed error (MSE), MAE, and MaxE for each ligand type and ultimately for the entire test set.

Dihydrogen Complexes. In general, as shown in Figure 4 and Table 1, the performance of ph-AFQMC is excellent for dihydrogen complexes (where the dihydrogen is the ligand being removed), including $[Ti(H_2)_4]^+$, $[Cu(H_2)_4]^+$, $[V(H_2)_4]^+$, $[V(H_2)_6]^+$, $[Co(H_2)_4]^+$, $[Ni(H_2)_4]^+$, $[Ti(H_2)_6]^+$, $[Co(H_2)_6]^+$, $[Fe(H_2)_6]^+$, $[Fe(H_2)_4]^+$, $Cr(CO)_5H_2$, $[Cr(H_2)_6]^+$, $[VH_2O(H_2)_3]^+$, and $[Cr(H_2)_4]^+$.

The relatively small system sizes of these dihydrogen complexes render the ph-AFQMC calculations affordable

https://dx.doi.org/10.1021/acs.jctc.0c00070
J. Chem. Theory Comput. 2020, 16, 3041−3054

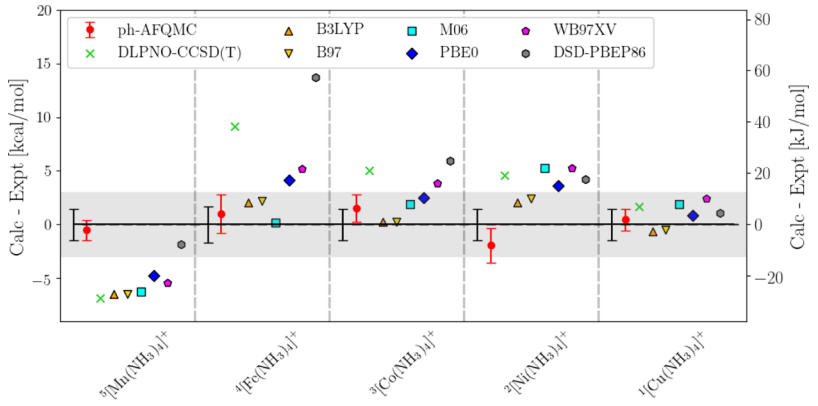

Figure 6. Deviations [kcal/mol on the left and kJ/mol on the right] of computational methods for the ammonia set of bond dissociation reactions. The multiplicities in the superscript at the start of the molecular formula apply for both reactant and dissociated product. The gray band indicates ±3 kcal/mol [12.5 kJ/mol] accuracy.

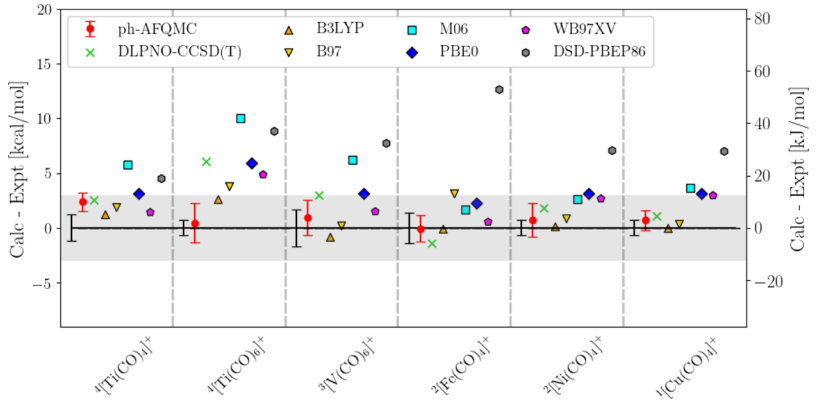

Figure 7. Deviations [kcal/mol on the left and kJ/mol on the right] of computational methods for the carbonyl set of bond dissociation reactions. The multiplicities in the superscript at the start of the molecular formula apply for both reactant and dissociated product, except for $^4[Fe(CO)_3]^+$. The gray band indicates ±3 kcal/mol [12.5 kJ/mol] accuracy.

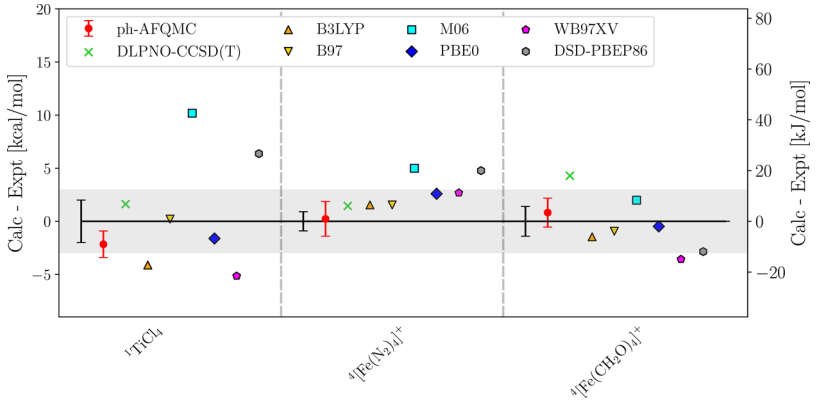

Figure 8. Deviations [kcal/mol on the left and kJ/mol on the right] of computational methods for the other reactions. The multiplicities in the superscript at the start of the molecular formula apply for both reactant and dissociated product, except for $^2TiCl_3$. The gray band indicates ±3 kcal/mol [12.5 kJ/mol] accuracy.

Table 1. MAEs, MSEs, and MaxEs [kcal/mol] for Dihydrogen Complexes[a]

	ph-AFQMC	CC	B3LYP	B97	M06	PBE0	ωB97X-V	DSD-PBEP86
MAE	0.85 ± 0.21	1.82	1.43	0.93	2.50	0.75	1.43	1.09
MSE	0.09 ± 0.21	1.75	−1.36	−0.67	1.94	0.33	1.08	1.04
MaxE	−1.51 ± 1.36	7.54	−3.29	−2.05	4.68	2.91	8.08	8.49

[a]The mean experimental uncertainty is 0.53 kcal/mol. CC refers to DLPNO-CCSD(T).

https://dx.doi.org/10.1021/acs.jctc.0c00070
J. Chem. Theory Comput. 2020, 16, 3041−3054

Table 2. MAEs, MSEs, and MaxEs [kcal/mol] for Aqua Complexes[a]

	ph-AFQMC	CC	B3LYP	B97	M06	PBE0	ωB97X-V	DSD-PBEP86
MAE	1.76 ± 0.85	3.22	2.24	2.13	5.17	2.72	3.76	3.33
MSE	0.58 ± 0.85	1.11	1.51	1.43	5.17	2.33	3.76	2.92
MaxE	2.96 ± 1.71	5.03	5.26	5.54	9.37	5.98	6.77	7.01

[a]The mean experimental uncertainty is 1.60 kcal/mol. CC refers to DLPNO-CCSD(T).

Table 3. MAEs, MSEs, and MaxEs [kcal/mol] for Ammonia Complexes[a]

	ph-AFQMC	CC	B3LYP	B97	M06	PBE0	ωB97X-V	DSD-PBEP86
MAE	1.95 ± 0.91	5.46	2.29	2.36	3.09	3.15	4.44	5.36
MSE	0.10 ± 0.91	2.71	−0.55	−0.42	0.60	1.25	2.26	4.61
MaxE	−1.95 ± 2.16	9.15	−6.48	−6.45	−6.22	−4.74	−5.45	13.69

[a]The mean experimental uncertainty is 1.48 kcal/mol. CC refers to DLPNO-CCSD(T).

Table 4. MAEs, MSEs, and MaxEs [kcal/mol] for Carbonyl Complexes[a]

	ph-AFQMC	CC	B3LYP	B97	M06	PBE0	ωB97X-V	DSD-PBEP86
MAE	0.87 ± 0.72	2.65	0.83	1.71	4.99	3.43	2.35	7.99
MSE	0.85 ± 0.72	2.18	0.52	1.71	4.99	3.43	2.35	7.99
MaxE	2.39 ± 1.46	6.07	2.64	3.80	10.02	5.90	4.88	12.68

[a]The mean experimental uncertainty is 1.06 kcal/mol. CC refers to DLPNO-CCSD(T).

even with the QZ basis set. Therefore, for $[Ni(H_2)_4]^+$, which showed deviations >2 kcal/mol (see the Supporting Information), we opted to do the full TZ/QZ extrapolation entirely within ph-AFQMC and found better agreement. In contrast, the scaling factor, that is, the ratio between the correlation energies computed by ph-AFQMC and DLPNO-CCSD(T) at the TZ level was close to or more than 1.3 for $[Co(H_2)_6]^+$ and $[Fe(H_2)_6]^+$, a metric found in our previous work,[40] so we also did TZ/QZ extrapolation entirely within ph-AFQMC in these cases, leading to good agreement. In the Supporting Information, we show that using ph-AFQMC/UHF to extrapolate gives similar results to the full treatment for the dihydrogen species.

M06 yields the largest MAE (2.5 kcal/mol) while B97, PBE0, and ph-AFQMC have MAEs less than 1 kcal/mol. Although ph-AFQMC and most DFs perform reasonably well for $Cr(CO)_5H_2$, especially given the relatively large experimental uncertainty, DSD-PBEP86 and DLPNO-CCSD(T) are off by 6−8 kcal/mol. We note that in the next section DSD-PBEP86 is seen to over-stabilize all carbonyl complexes. ωB97X-V drastically overestimates the BDE of the $[Ni(H_2)_4]^+$ complex, with a deviation of 8.08 kcal/mol. Indeed, as will be shown, this functional over-stabilizes all Ni complexes.

Aqua Complexes. As shown in Figure 5 and Table 2, ph-AFQMC also yields accurate results for the hexa-aqua complex $[Ni(H_2O)_6]^{2+}$ and the tetra-aqua complexes $[Cr(H_2O)_4]^+$, $[Ni(H_2O)_4]^+$, $[Ti(H_2O)_4]^+$, $[V(H_2O)_4]^+$, and $[Fe(H_2O)_4]^+$. Although all other methods seem to overbind these complexes, as can be seen by large and positive MSEs, ph-AFQMC appears to predict the BDEs in a relatively balanced manner.

In the case of $[Ni(H_2O)_6]^{2+}$, the scaling factor was below 0.6, which indicates a poor match between the correlation energies of ph-AFQMC and DLPNO-CCSD(T). As full TZ/QZ extrapolation within ph-AFQMC was unaffordable in the present version of our code implementation because of prohibitively high required device memory, we opted to do the extrapolation with a single-determinant (UHF) trial-based QMC in place of DLPNO-CCSD(T) and found good results. Similarly, we performed the extrapolation with ph-AFQMC/UHF for $[V(H_2O)_4]^+$, on the basis of disagreement of experiment rather than the scaling factor, and found that the deviation went from 4.03 ± 1.95 kcal/mol with the DLPNO-CCSD(T) extrapolation to 1.35 ± 2.38 kcal/mol with the ph-AFQMC/UHF extrapolation. The other methods have errors around 5−9 kcal/mol for this molecule.

On average, as seen in Table 2, the accuracy of CC and DFT methods for metal-aqua complexes is similar with MAEs between 2.13 (B97) and 5.17 (M06) kcal/mol. The MAE of ph-AFQMC is 1.76 ± 0.85 kcal/mol, with a MaxE of 2.96 ± 1.71 kcal/mol found for the $[Ni(H_2O)_4]^+$ species. We note that all methods overestimate the BDE of this molecule, although not by a huge amount, especially in light of the experimental error bars. The experimental value for this case should be investigated further.

Ammonia Complexes. Figure 6 and Table 3 summarize the performance of the computational methods for the tetraammonia complexes: $[Co(NH_3)_4]^+$, $[Ni(NH_3)_4]^+$, $[Mn(NH_3)_4]^+$, $[Cu(NH_3)_4]^+$, and $[Fe(NH_3)_4]^+$.

$[Mn(NH_3)_4]^+$ is a difficult case for all methods. DSD-PBEP86 and ph-AFQMC, with deviations of ∼2 kcal/mol, performed better compared to other methods, which showed errors of ∼6 kcal/mol. This reaction involves the only two molecules {i.e., $[Mn(NH_3)_4]^+$ and $[Mn(NH_3)_3]^+$} where we had to run separate ph-AFQMC calculations with population control because the imaginary trajectories were not convincingly equilibrated by 15 E_h^{-1}. Additionally, there were many CAS convergence issues that prevented us from running larger CASSCF active spaces to check the convergence. Further investigation will be required. DLPNO-CCSD(T) and the remaining DFs perform particularly poorly for this molecule with errors around or above 4.7 kcal/mol, except for DSD-PBEP86, which interestingly is within the 2 kcal/mol of the experimental value.

We note that $[Ni(NH_3)_4]^+$ is another case for which basis set extrapolation with ph-AFQMC/UHF reduced the deviation from experiment.

In terms of alternate experimental values from Rodgers and Armentrout,[52] there are two measured values for [Cu-

https://dx.doi.org/10.1021/acs.jctc.0c00070
J. Chem. Theory Comput. 2020, 16, 3041−3054

Table 5. MAEs, MSEs, and MaxEs [kcal/mol] for Miscellaneous Complexes[a]

	ph-AFQMC	CC	B3LYP	B97	M06	PBE0	ωB97X-V	DSD-PBEP86
MAE	1.07 ± 1.19	2.45	2.37	0.89	5.72	1.56	3.80	4.66
MSE	−0.37 ± 1.19	2.45	−1.35	0.27	5.72	0.17	−2.01	2.76
MaxE	−2.16 ± 2.36	4.29	−4.12	1.54	10.18	2.59	−5.15	6.37

[a]The mean experimental uncertainty is 1.43 kcal/mol. CC refers to DLPNO-CCSD(T).

$(NH_3)_4]^+$: 10.0 ± 1.4 kcal/mol, measured by TCID[82] and which we use, and an older value of 12.18 ± 0.24, measured by high-pressure temperature-dependent equilibrium.[83] We find better agreement of the former value with ph-AFQMC, suggesting that the TCID approach is more reliable.

Overall, ph-AFQMC, B3LYP, B97, and M06 have notably small MSEs. ph-AFQMC performs remarkably well here with respect to MAE (1.95 ± 0.91 kcal/mol) and MaxE (−1.95 ± 2.16 kcal/mol) while other methods show an absolute MaxE around 5−14 kcal/mol for these complexes. DLPNO-CCSD(T) and DSD-PBEP86 showed the largest deviations, with MAEs of 5.46 and 5.36 kcal/mol, respectively. They show extreme errors for $[Fe(NH_3)_4]^+$ in particular, with MaxEs of 9 and 14 kcal/mol, respectively.

Carbonyl Complexes. As shown in Figure 7 and Table 4, ph-AFQMC also performed well for the species with all carbonyl ligands: $[Ti(CO)_6]^+$, $[Ni(CO)_4]^+$, $[Cu(CO)_4]^+$, $[Ti(CO)_4]^+$, $[Fe(CO)_4]^+$, and $[V(CO)_6]^+$. In particular, ph-AFQMC is the only method to predict a BDE close to the experimental value for $[Ti(CO)_6]^+$ aside from B3LYP, which produces a result just within 3 kcal/mol of the experimental value.

DSD-PBEP86 gives an extremely large deviation of 12.68 kcal/mol for $[Fe(CO)_4]^+$ and in fact overpredicts all carbonyl species in this set, with an MAE and MSE of ∼7.99 kcal/mol. M06 has the second largest MAE (4.99 kcal/mol) and MaxE (10.02 kcal/mol for $[Ti(CO)_6]^+$) among all methods. For these carbonyl complexes, both ph-AFQMC and B3LYP showed outstanding performance with balanced predictions (low MSEs), MAEs of <1 kcal/mol, and MaxEs of ∼2.5 kcal/mol.

In the case of $[Ti(CO)_4]^+$, all methods predict BDEs above the experimental measurement. The experimental value for this case should also be investigated further. In terms of alternate experimental values from Rodgers and Armentrout,[52] there is a TCID measurement for $[Fe(CO)_4]^+$, yielding a value of 23.3 ± 1.4 kcal/mol,[84,85] and a photoionization threshold measurement (PI), yielding a value of 25.1 ± 1.2 kcal/mol.[86,87] Similarly, there are two measurements for $[Ni(CO)_4]^+$ which yield values of 17.2 ± 0.70 kcal/mol (TCID)[88] and 16.3 ± 0.5 kcal/mol (PI).[86] For both reactions, we find better agreement between the TCID value and ph-AFQMC, once again strongly suggesting that this method is more reliable.

Miscellaneous Complexes. As can be seen in Figure 8, ph-AFQMC continues to predict consistently accurate BDEs for these three complexes. Although a statistical analysis of three compounds is likely not rigorously meaningful, we nonetheless provide a summary in Table 5 for completeness.

The experimental uncertainty corresponding to the measured $TiCl_4$ BDE is the highest among the molecules included in this study, at 2 kcal/mol. Most of the methods give reasonable performance except DSD-PBEP86, M06, and ωB97X-V. The first two overestimated the BDE by ∼6−10 kcal/mol while the latter underestimated it by 5.15 kcal/mol.

We note that all DFT methods overestimate the BDE of $[Fe(N_2)_4]^+$, with M06 and DSD-PBEP86 yielding deviations of around 5 kcal/mol.

The formaldehyde ligands make $[Fe(CH_2O)_4]^+$ the largest molecule studied in this work. ωB97X-V and DSD-PBEP86 yield deviations of ∼−3 kcal/mol while DLPNO-CCSD(T) yields of a deviation around ∼3 kcal/mol.

Performance for the Entire Test Set. The statistical performance of each computational method over all ligand types is summarized in Table 6. We note that the average experimental uncertainty is 1.05 kcal/mol.

Table 6. MAEs, MSEs, and MaxEs [kcal/mol] of Ph-AFQMC, DLPNO-CCSD(T), and DFT Results and Other Methods for the 34 Molecule Set Shown in Figure 1[a]

	MAE	MSE	MaxE
ph-AFQMC	1.07 ± 0.27	0.27 ± 0.27	2.96 ± 1.71
B97	1.49	0.24	−6.45
B3LYP	1.67	−0.40	−6.48
PBE0	1.99	1.35	5.98
ωB97X-V	2.65	1.68	8.08
DLPNO-CCSD(T)	2.81	1.91	9.15
DSD-PBEP86/2013	3.65	3.27	13.69
M06	3.78	3.19	10.18

[a]The values are sorted by MAE. The ph-AFQMC deviations incorporate both the experimental uncertainty and the statistical uncertainty.

ph-AFQMC, B97, and B3LYP have near-zero MSEs while all other methods systematically overestimate the BDEs. ph-AFQMC outperforms all DFT functionals and DLPNO-CCSD(T), with an MAE of 1.07 ± 0.27 kcal/mol and MaxE of 2.96 ± 1.71 kcal/mol. DLPNO-CCSD(T) performs worse than most of the hybrid functionals in the study, with MAE and MaxE of 2.81 and 9.15 kcal/mol, respectively. In light of the average uncertainty in the experimental measurements reported above, the B97 and B3LYP functionals arguably yield, on average, comparable accuracy to ph-AFQMC, with MAEs of 1.49 and 1.67 kcal/mol, respectively. However, the MaxEs of −6.45 and −6.48 kcal/mol are more than twice as large as that from ph-AFQMC and would be considered much too large for many predictive applications. ωB97X-V achieved a similar accuracy as DLPNO-CCSD(T), with MAE and MaxE of 2.65 and 5.98 kcal/mol, respectively. This performance is rather satisfactory given that there were no transition metals in the training set used to fit the 10 empirical parameters in the functional.[16] In contrast, the Minnesota functional, M06, is heavily parameterized and results in the largest MAE of 3.78 kcal/mol. The poor performance of M06 for transition-metal complexes was also mentioned in our group's previous paper[89] and in the work of Steinmetz and Grimme.[32] In contrast to the high accuracy achieved by double-hybrid functionals for organic molecules,[80,81] the DSD-PBEP86 functional for this

https://dx.doi.org/10.1021/acs.jctc.0c00070
J. Chem. Theory Comput. 2020, 16, 3041−3054

dataset yielded an MAE of 3.65 kcal/mol and MaxE of 13.69 kcal/mol.

As observed by many groups, including those of Martin and co-workers and Steinmetz and Grimme, DFs with a smaller amount of HF exchange tend to perform better than those with larger percentages.[31,32] We see a similar trend that B97 (19.43% HF exchange) gives the best performance for this dataset while M06 (27% HF exchange) and DSD-PBEP86 (~70% HF exchange) perform the worst. PBE0 with an MAE of 2.17 kcal/mol is slightly worse than B3LYP and B97; however, it yields good results for dihydrogen complexes. Presumably, this is because of the difficulty that HF and MP2 methods have in dealing with the static correlation found in transition metals as discussed by Harvey in ref 90.

We attempted to correlate a number of multireference diagnostics, such as the fractional occupation number weighted electron density (FOD)[91,92] and the square of the leading CI coefficient in the CASSCF calculation,[46] with errors from DLPNO-CCSD(T). However, no significant correlation was found. This is consistent with previous studies reporting similar inefficacy for transition-metal systems.[36−39,46] We emphasize the need for further investigation and development of multireference diagnostics that can reliably identify the presence of strong correlation effects and thus signal caution to users of single-reference methods such as DFT and CCSD(T). One promising approach involves examining the deviation of $\langle S^2_{UHF}\rangle$ from spin-pure values, in conjunction with the use of an orbital-optimized method, for example, MP*n*, to rule out artificial symmetry breaking.[93]

For reactions involving Sc, Ti, V, and Cr centers, our ph-AFQMC results are typically in good agreement with experiment even when relatively small active spaces are employed in the trial wave function. Such calculations need only use the MINAO basis set to specify the 3d orbitals as inputs for the AVAS procedure for selecting the active space. For the remaining metals, larger active spaces (i.e., including higher-lying virtual orbitals) are required and we, therefore, used the ANO-RCC basis for AVAS, specifying both the 3d and 4d atomic orbitals to account for the double-shell effect.[50,94,95]

As a number of functionals were trained utilizing larger basis sets than the one employed in this work, we note that the results may change slightly if such optimal basis sets had been employed. We did investigate the basis set dependence for the double-hybrid functional, as the MP2-like part is known to perform better with a basis larger than TZ to more closely approach the CBS limit.[96,97] We found for the largest outliers for DSD-PBEP86 that using a QZ basis set for the single-point energy calculations did not significantly change the results. For example, the calculated BDEs of $[Fe(NH_3)_4]^+$ in TZ and QZ deviate from experiment by 13.69 and 13.89 kcal/mol, respectively.

DISCUSSION

The results we have obtained lead to interesting observations concerning all three classes of approaches considered in this paper: ph-AFQMC, DLPNO-CCSD(T), and DFT. These observations have implications that go beyond the current data set. Our previous ph-AFQMC study on transition metal-containing diatomics[40] could be viewed as addressing a very special subset of unusual and difficult molecules from an electronic structure point of view. In particular, these systems are coordinatively unsaturated, with nearly degenerate electronic states in a number of cases, and of a form rarely present in important chemical systems relevant to practical applications in biology and materials science. In contrast, the present data set contains many typical bonding motifs, namely four- and six-coordinated metal−ligand complexes, although the oxidation states are lower than is usually found in condensed phase systems. Arguably, a system such as the water-splitting complex in PSII poses a much more difficult quantum chemistry problem than the molecules considered here. A method that displays a significant number of outliers in our present data set would be difficult to trust as reliable if applied to a strongly interacting, multimetal complex with a large number of low-lying electronic states.

The ph-AFQMC results satisfy all of the criteria one could reasonably expect (given the uncertainties in the experimental data) for true benchmark performance. The largest deviation from experiment is less than 3 kcal/mol, often cited as the target for "transition-metal chemical accuracy"[73] and close to being within the cited experimental error bars. For most of the ligands studied, the maximum deviation is closer to 2 kcal/mol and well within the experimental error. Results reliably improve (sometimes considerably) as the quality of the calculation is increased, for example, via an upgrade in the basis set extrapolation method. In fact, the error for the $[Ni(H_2O)_4]^+$ molecule, which represents the MaxE of ph-AFQMC in Table 6, can be reduced to less than 1 kcal/mol when utilizing QMC/UHF rather than DLPNO-CCSD(T) for the basis set extrapolation (we indicate in Tables S4 and S5 that extrapolating with QMC/UHF will produce equally good if not better final BDEs for a representative selection of molecules, suggesting that such extrapolation is to be preferred, if computationally feasible, in future studies). With this update, the MaxE of ph-AFQMC would be lowered to 2.39 ± 1.46 kcal/mol, for $[Ti(CO)_4]^+$, which is a rather outstanding result in light of the experimental uncertainty. The overall mean unsigned deviation from the experiment of 1.1 kcal/mol is highly satisfactory. It is in fact not obvious how much of this deviation is due to errors in the theory and how much to errors in the experiment. In our transition-metal diatomic publication, it is noteworthy that when new (and more reliable) experiments were released after the calculations were completed (but prior to publication), agreement of ph-AFQMC with these results was significantly better than with older values. In the absence of significantly more accurate experiments, it is hard to imagine a better performance from a tractable theoretical approach.

The DLPNO-CCSD(T) results, in contrast, reveal a large number of major outliers (with a maximum outlier of 9.15 kcal/mol) across every single ligand series (maximum deviations for the individual series range from 4.29 to 9.15 kcal/mol). The DLPNO approximations, in particular, that (a) the correlation energy of the system can be written as a sum of pair energies arising from the correlation between electrons in two occupied localized orbitals, and (b) the "domain" of virtual orbitals considered for each pair of occupied orbitals can be truncated to include only those that are spatially and energetically close, are likely not the most significant sources of error, given that we use the tightest possible cutoff parameters. Recent results[43,98,99] show that DLPNO-CCSD(T) and similar methods recover 99.86% of the CC correlation energy for large organic systems with similar performance for the transition metal-containing oxygenase, lending support to this statement.[100] In addition, because of the relatively small

https://dx.doi.org/10.1021/acs.jctc.0c00070
J. Chem. Theory Comput. 2020, 16, 3041−3054

size of the dissociating ligand, it is reasonable to expect some degree of cancellation in the localization errors. It is most likely that excitations of higher order than (T) are required for consistently high accuracy, although we note that it would be useful in future work to probe the effects of utilizing orbitals from, for example, an unrestricted DFT calculation or other orbitals, as in the work of Dixon and co-workers.[101,102] Regardless of the source of the errors, the implication is that much more expensive (and poorly scaling) variants of coupled cluster will be needed to converge this approach to chemical accuracy for transition metal-containing systems. Now that benchmark values are available (via our ph-AFQMC results) for both transition metal-containing diatomics and small four- and six-coordinated complexes (comprising roughly 80 systems in all), we look forward to alternative CC approximations, particularly using CCSD(T), being rigorously evaluated using these data. At that point, assuming that comparable benchmark quality can be achieved, it will be interesting to compare the computational requirements, and scaling with system size, of both methods. Nonetheless, these specific types of transition-metal systems, and the ligand-dissociation reactions involved, have not been comprehensively tested with DLPNO-CCSD(T), and thus, in principle, the approximations within DLPNO could lead to differences with full CCSD(T). Therefore, strictly speaking, our assessment of CCSD(T) is limited to the particular implementation we ran.

The DFT results shown here are far from a comprehensive survey of the various flavors of functionals currently available but do contain a number of qualitatively different functionals as well as several of the most widely used approaches. A striking observation is that the three best performing functionals—by a considerable margin—were published more than 20 years ago. Despite the use of considerably more sophisticated functional forms, the performance of the three more recent functionals (wB97X-V, DSD-PBDP86, and M06) has substantially worse average errors and larger and more frequent outliers, than the older approaches. It should also be noted that the best performing DFT approaches work substantially better than DLPNO-CCSD(T). This observation is in accordance with the proposition put forth along these lines by Truhlar and co-workers several years ago, which has been the subject of considerable controversy in the literature.[36,39,40] Although one could ultimately converge coupled cluster-based methods to a benchmark level of accuracy by including higher (and considerably more expensive) levels of theory, what is going to be necessary and sufficient to accomplish that convergence is apparently more demanding than some of the earlier papers in this debate have suggested.

Our results cast doubt as to whether the newer DFT models use a functional form that is an actual improvement from the point of view of transition-metal chemistry, as the incorporation of asymptotically correct exchange, nonlocal correlation, MP2 contributions, kinetic energy density-dependence and/or a greater number of parameters appears not to yield improved accuracy over simpler hybrid GGA forms. As in the case of typical machine learning problems, consideration of additional parameters generally leads to better performance when the test cases are similar to the molecules in the training set, that is, when direct interpolation is performed. Extrapolation outside of the training set, however, is a very different proposition. The lack of confidence in the experimental values for transition-metal energetics has deterred extensive incorporation of data of the type we have studied here into the process of fitting DFT functionals. Our benchmark level of agreement with experiment should enable new efforts, incorporating the data we have validated here, to proceed with more confidence. Also, it is of course possible that one of the many DFT functionals that we have not tested in this paper would improve upon any of the results presented above. Again, data are now available to rigorously interrogate such a proposition.

The performance of the two best performing methods, B3LYP and B97, is quite remarkable, considering their vintage and relatively small number of fitting parameters (3 and 10, respectively). It is interesting that whereas B97 was clearly superior for the transition-metal diatomic data set, the results for the present data set are much closer in average and MaxE. For calculations of large, transition metal-containing systems, we would view either of these alternatives as the best currently available, particularly given the extensive experience with them over the past several decades (although not of benchmark quality, in view of the presence of a significant number of outliers in the 3−7 kcal/mol error range). If the ph-AFQMC calculations can be scaled up to address systems with 50−100 atoms, perhaps by using localized orbital techniques, a combination of ph-AFQMC benchmarks, followed by B97 or B3LYP modeling of a larger set of conformations (including environmental effects such as solvation), could provide a path toward calculations of high enough quality to understand reaction mechanisms, identify intermediates, and contribute to molecular design efforts.

CONCLUSIONS

Our ph-AFQMC approach has produced reliable theoretical values for BDEs in 3d transition-metal coordination complexes. Our results demonstrate that future, predictive benchmarking should employ CAS trial wave functions in the TZ basis with QMC/UHF for CBS extrapolation. The MAEs of the DFs considered in this study are in general quite satisfactory, but the occasional presence of large, unsystematic errors leaves cause for concern. The performance of methods by MAE from best to worst is ph-AFQMC, B97, B3LYP, PBE0, DLPNO-CCSD(T), ωB97X-V, DSD-PBEP86, and M06.

We envision that this dataset of gas-phase BDEs may prove useful for the development of new approximate methods and new DFs. The reliability of the ph-AFQMC method, namely its ability to compute accurate gas-phase energetics in a reasonable amount of wall-time, will enable the development of accurate force fields for metal ion interactions with various ligands. The method will also help in a forthcoming investigation of DFT ability to predict solution-phase properties. For instance, we are now in a position to answer the question: are errors found in recent studies of aqueous pK_a's[12] and redox potentials[89] due inherently to deficiencies in the quantum-chemical electronic structure description or in the implicit solvent models employed, or both?

For the systems in this work, we were generally able to converge the BDEs with respect to active space size of the trial wave functions. However, moving on to larger systems, perhaps containing multiple metals or bulky ligands, we anticipate that the relevant active space sizes will outpace the limits of conventional CASSCF algorithms and available computing resources. Investigations along these lines are currently underway, as are efforts to implement a localized orbital approach to ph-AFQMC.

https://dx.doi.org/10.1021/acs.jctc.0c00070
J. Chem. Theory Comput. 2020, 16, 3041−3054

■ ASSOCIATED CONTENT

Supporting Information

The Supporting Information is available free of charge at https://pubs.acs.org/doi/10.1021/acs.jctc.0c00070.

Tabulated ph-AFQMC BDEs and statistical uncertainties resulting from CBS extrapolations via DLPNO-CCSD(T), UHF-trial ph-AFQMC, and CAS-trial ph-AFQMC, scaling factors for the CBS extrapolations, active space sizes, AVAS thresholds, multiplicities, justification of the active space chosen for the free-standing ligands, tabulated experimental (including references for each data point), DFT, and DLPNO-CCSD(T) data, control studies for the CBS extrapolations using ph-AFQMC with UHF trial wave functions, additional details for the ORCA calculations, how CBS extrapolations are done for DLPNO-CCSD(T) and for ph-AFQMC, a workflow in terms of how other calculations complement the ph-AFQMC calculations, and glossary of commonly used terms for ph-AFQMC (PDF)

B3LYP-optimized coordinates for transition-metal complexes (TXT)

■ AUTHOR INFORMATION

Corresponding Author

James Shee − *Department of Chemistry, Columbia University, New York, New York 10027, United States;* orcid.org/0000-0001-8333-8151; Email: js4564@columbia.edu

Authors

Benjamin Rudshteyn − *Department of Chemistry, Columbia University, New York, New York 10027, United States;* orcid.org/0000-0002-9511-6780

Dilek Coskun − *Department of Chemistry, Columbia University, New York, New York 10027, United States*

John L. Weber − *Department of Chemistry, Columbia University, New York, New York 10027, United States;* orcid.org/0000-0002-4937-9651

Evan J. Arthur − *Schrodinger Inc., New York, New York 10036, United States*

Shiwei Zhang − *Center for Computational Quantum Physics, Flatiron Institute, New York, New York 10010, United States; Department of Physics, College of William and Mary, Williamsburg, Virginia 23187, United States*

David R. Reichman − *Department of Chemistry, Columbia University, New York, New York 10027, United States*

Richard A. Friesner − *Department of Chemistry, Columbia University, New York, New York 10027, United States;* orcid.org/0000-0002-1708-9342

Complete contact information is available at: https://pubs.acs.org/10.1021/acs.jctc.0c00070

Author Contributions

⊥B.R. and D.C. made equal contributions.

Notes

The authors declare no competing financial interest.

■ ACKNOWLEDGMENTS

D.R.R. acknowledges funding from NSF CHE-1839464. S.Z. acknowledges funding from DOE DE-SC0001303. This research used resources of the Oak Ridge Leadership Computing Facility at the Oak Ridge National Laboratory, which is supported by the Office of Science of the U.S. Department of Energy under contract no. DE-AC05-00OR22725. This work used the Extreme Science and Engineering Discovery Environment (XSEDE), which is supported by National Science Foundation grant number ACI-1548562. In particular, we used San Diego Computing Center's Comet resources under grant number TG-CHE190007 and allocation ID COL151. The Flatiron Institute is a division of the Simons Foundation. We would like to thank Elvira Sayfutyarova for helpful discussions regarding AVAS.

■ REFERENCES

(1) Prier, C. K.; Rankic, D. A.; MacMillan, D. W. C. Visible Light Photoredox Catalysis With Transition Metal Complexes: Applications in Organic Synthesis. *Chem. Rev.* **2013**, *113*, 5322−5363.

(2) Trautwein, A. *Bioinorganic Chemistry: Transition Metals in Biology and Their Coordination Chemistry*; Wiley-VCH, 1997.

(3) Khomskii, D. *Transition Metal Compounds*; Cambridge University Press, 2014.

(4) Siegbahn, P. E. M. Nucleophilic Water Attack Is Not a Possible Mechanism for O-O Bond Formation in Photosystem II. *Proc. Natl. Acad. Sci. U.S.A.* **2017**, *114*, 4966.

(5) Raugei, S.; Seefeldt, L. C.; Hoffman, B. M. Critical Computational Analysis Illuminates the Reductive-Elimination Mechanism That Activates Nitrogenase for N_2 Reduction. *Proc. Natl. Acad. Sci. U.S.A.* **2018**, *115*, E10521−E10530.

(6) Askerka, M.; Brudvig, G. W.; Batista, V. S. The O_2-Evolving Complex of Photosystem II: Recent Insights from Quantum Mechanics/Molecular Mechanics (QM/MM), Extended X-ray Absorption Fine Structure (EXAFS), and Femtosecond X-ray Crystallography Data. *Acc. Chem. Res.* **2016**, *50*, 41−48.

(7) Siegbahn, P. E. M. Nucleophilic water attack is not a possible mechanism for O-O bond formation in photosystem II. *Proc. Natl. Acad. Sci. U.S.A.* **2017**, *114*, 4966−4968.

(8) Riccardi, L.; Genna, V.; De Vivo, M. Metal-ligand interactions in drug design. *Nat. Rev. Chem.* **2018**, *2*, 100−112.

(9) Lee, P. A.; Nagaosa, N.; Wen, X.-G. Doping a Mott Insulator: Physics of High-Temperature Superconductivity. *Rev. Mod. Phys.* **2006**, *78*, 17.

(10) Dagotto, E. Correlated Electrons in High-Temperature Superconductors. *Rev. Mod. Phys.* **1994**, *66*, 763.

(11) Friesner, R. A. Modeling Metalloenzymes with Density Functional and Mixed Quantum Mechanical/Molecular Mechanical (QM/MM) Calculations: Progress and Challenges. *Encyclopedia of Inorganic and Bioinorganic Chemistry*; John Wiley and Sons, Inc., 2011.

(12) Jerome, S. V.; Hughes, T. F.; Friesner, R. A. Successful Application of the DBLOC Method to the Hydroxylation of Camphor by Cytochrome p450. *Protein Sci.* **2016**, *25*, 277−285.

(13) Rudshteyn, B.; Fisher, K. J.; Lant, H. M. C.; Yang, K. R.; Mercado, B. Q.; Brudvig, G. W.; Crabtree, R. H.; Batista, V. S. Water-Nucleophilic Attack Mechanism for the $Cu^{II}(pyalk)_2$ Water-Oxidation Catalyst. *ACS Catal.* **2018**, *8*, 7952−7960.

(14) Agarwal, J.; Fujita, E.; Schaefer, H. F., III; Muckerman, J. T. Mechanisms for CO Production From CO_2 Using Reduced Rhenium Tricarbonyl Catalysts. *J. Am. Chem. Soc.* **2012**, *134*, 5180−5186.

(15) Han, J. L.; You, J.; Yonemura, H.; Yamada, S.; Wang, S. R.; Li, X. G. Metallophthalocyanines as triplet sensitizers for highly efficient photon upconversion based on sensitized triplet-triplet annihilation. *Photochem. Photobiol. Sci.* **2016**, *15*, 1039−1045.

(16) Mardirossian, N.; Head-Gordon, M. ωB97X-V: A 10-parameter, range-separated hybrid, generalized gradient approximation density functional with nonlocal correlation, designed by a survival-of-the-fittest strategy. *Phys. Chem. Chem. Phys.* **2014**, *16*, 9904−9924.

(17) Mardirossian, N.; Head-Gordon, M. ωB97M-V: A combinatorially optimized, range-separated hybrid, meta-GGA density functional with VV10 nonlocal correlation. *J. Chem. Phys.* **2016**, *144*, 214110.

(18) Marenich, A. V.; Cramer, C. J.; Truhlar, D. G. Universal Solvation Model Based on Solute Electron Density and on a Continuum Model of the Solvent Defined by the Bulk Dielectric Constant and Atomic Surface Tensions. *J. Phys. Chem. B* **2009**, *113*, 6378−6396.
(19) Bross, D. H.; Hill, J. G.; Werner, H.-J.; Peterson, K. A. Explicitly Correlated Composite Thermochemistry of Transition Metal Species. *J. Chem. Phys.* **2013**, *139*, 094302.
(20) Manivasagam, S.; Laury, M. L.; Wilson, A. K. Pseudopotential-Based Correlation Consistent Composite Approach (rp-ccCA) for First- and Second-Row Transition Metal Thermochemistry. *J. Phys. Chem. A* **2015**, *119*, 6867−6874.
(21) Jiang, W.; Laury, M. L.; Powell, M.; Wilson, A. K. Comparative Study of Single and Double Hybrid Density Functionals for the Prediction of 3d Transition Metal Thermochemistry. *J. Chem. Theor. Comput.* **2012**, *8*, 4102−4111.
(22) Zhang, W.; Truhlar, D. G.; Tang, M. Tests of Exchange-Correlation Functional Approximations Against Reliable Experimental Data for Average Bond Energies of 3d Transition Metal Compounds. *J. Chem. Theory Comput.* **2013**, *9*, 3965−3977.
(23) Moltved, K. A.; Kepp, K. P. Chemical Bond Energies of 3d Transition Metals Studied by Density Functional Theory. *J. Chem. Theory Comput.* **2018**, *14*, 3479.
(24) Jiang, W.; DeYonker, N. J.; Determan, J. J.; Wilson, A. K. Toward Accurate Theoretical Thermochemistry of First Row Transition Metal Complexes. *J. Phys. Chem. A* **2011**, *116*, 870−885.
(25) Carlson, R. K.; Li Manni, G.; Sonnenberger, A. L.; Truhlar, D. G.; Gagliardi, L. Multiconfiguration Pair-Density Functional Theory: Barrier Heights and Main Group and Transition Metal Energetics. *J. Chem. Theor. Comput.* **2014**, *11*, 82−90.
(26) Bao, J. L.; Odoh, S. O.; Gagliardi, L.; Truhlar, D. G. Predicting Bond Dissociation Energies of Transition-Metal Compounds by Multiconfiguration Pair-Density Functional Theory and Second-Order Perturbation Theory Based on Correlated Participating Orbitals and Separated Pairs. *J. Chem. Theory Comput.* **2017**, *13*, 616−626.
(27) Bao, J. L.; Zhang, X.; Xu, X.; Truhlar, D. G. Predicting Bond Dissociation Energy and Bond Length for Bimetallic Diatomic Molecules: A Challenge for Electronic Structure Theory. *Phys. Chem. Chem. Phys.* **2017**, *19*, 5839−5854.
(28) Sharkas, K.; Gagliardi, L.; Truhlar, D. G. Multiconfiguration Pair-Density Functional Theory and Complete Active Space Second Order Perturbation Theory. Bond Dissociation Energies of FeC, NiC, FeS, NiS, FeSe, and NiSe. *J. Phys. Chem. A* **2017**, *121*, 9392−9400.
(29) Tran, L. N.; Iskakov, S.; Zgid, D. Spin-Unrestricted Self-Energy Embedding Theory. *J. Phys. Chem. Lett.* **2018**, *9*, 4444.
(30) Bartlett, R. J.; Musiał, M. Coupled-Cluster Theory in Quantum Chemistry. *Rev. Mod. Phys.* **2007**, *79*, 291.
(31) Quintal, M. M.; Karton, A.; Iron, M. A.; Boese, A. D.; Martin, J. M. L. Benchmark Study of DFT Functionals for Late-Transition-Metal Reactions. *J. Phys. Chem. A* **2006**, *110*, 709−716.
(32) Steinmetz, M.; Grimme, S. Benchmark Study of the Performance of Density Functional Theory for Bond Activations with (Ni,Pd)-Based Transition-Metal Catalysts. *ChemistryOpen* **2013**, *2*, 115−124.
(33) Kang, R.; Lai, W.; Yao, J.; Shaik, S.; Chen, H. How Accurate Can a Local Coupled Cluster Approach Be in Computing the Activation Energies of Late-Transition-Metal-Catalyzed Reactions With Au, Pt, and Ir? *J. Chem. Theory Comput.* **2012**, *8*, 3119−3127.
(34) Dohm, S.; Hansen, A.; Steinmetz, M.; Grimme, S.; Checinski, M. P. Comprehensive Thermochemical Benchmark Set of Realistic Closed-Shell Metal Organic Reactions. *J. Chem. Theory Comput.* **2018**, *14*, 2596−2608.
(35) Chan, B.; Gill, P. M. W.; Kimura, M. Assessment of DFT Methods for Transition Metals with the TMC151 Compilation of Data Sets and Comparison with Accuracies for Main-Group Chemistry. *J. Chem. Theory Comput.* **2019**, *15*, 3610.
(36) Xu, X.; Zhang, W.; Tang, M.; Truhlar, D. G. Do Practical Standard Coupled Cluster Calculations Agree Better than Kohn-Sham Calculations with Currently Available Functionals When Compared to the Best Available Experimental Data for Dissociation Energies of Bonds to 3d Transition Metals? *J. Chem. Theory Comput.* **2015**, *11*, 2036−2052.
(37) Cheng, L.; Gauss, J.; Ruscic, B.; Armentrout, P. B.; Stanton, J. F. Bond Dissociation Energies for Diatomic Molecules Containing 3d Transition Metals: Benchmark Scalar-Relativistic Coupled-Cluster Calculations for 20 Molecules. *J. Chem. Theory Comput.* **2017**, *13*, 1044−1056.
(38) Fang, Z.; Vasiliu, M.; Peterson, K. A.; Dixon, D. A. Prediction of Bond Dissociation Energies/Heats of Formation for Diatomic Transition Metal Compounds: CCSD(T) Works. *J. Chem. Theory Comput.* **2017**, *13*, 1057−1066.
(39) Aoto, Y. A.; de Lima Batista, A. P.; Köhn, A.; de Oliveira-Filho, A. G. S. How to Arrive at Accurate Benchmark Values for Transition Metal Compounds: Computation or Experiment? *J. Chem. Theory Comput.* **2017**, *13*, 5291−5316.
(40) Shee, J.; Rudshteyn, B.; Arthur, E. J.; Zhang, S.; Reichman, D. R.; Friesner, R. A. On Achieving High Accuracy in Quantum Chemical Calculations of 3d Transition Metal-Containing Systems: A Comparison of Auxiliary-Field Quantum Monte Carlo with Coupled Cluster, Density Functional Theory, and Experiment for Diatomic Molecules. *J. Chem. Theory Comput.* **2019**, *15*, 2346−2358.
(41) Williams, K. T.; et al. Direct Comparison of Many-Body Methods for Realistic Electronic Hamiltonians. *Phys. Rev. X* **2020**, *10*, 011041.
(42) Hait, D.; Tubman, N. M.; Levine, D. S.; Whaley, K. B.; Head-Gordon, M. What Levels of Coupled Cluster Theory Are Appropriate for Transition Metal Systems? A Study Using Near-Exact Quantum Chemical Values for 3d Transition Metal Binary Compounds. *J. Chem. Theory Comput.* **2019**, *15*, 5370−5385.
(43) Guo, Y.; Riplinger, C.; Becker, U.; Liakos, D. G.; Minenkov, Y.; Cavallo, L.; Neese, F. Communication: An Improved Linear Scaling Perturbative Triples Correction for the Domain Based Local Pair-Natural Orbital Based Singles and Doubles Coupled Cluster Method [DLPNO-CCSD(T)]. *J. Chem. Phys.* **2018**, *148*, 011101.
(44) Riplinger, C.; Pinski, P.; Becker, U.; Valeev, E. F.; Neese, F. Sparse maps-A systematic infrastructure for reduced-scaling electronic structure methods. II. Linear scaling domain based pair natural orbital coupled cluster theory. *J. Chem. Phys.* **2016**, *144*, 024109.
(45) Husch, T.; Freitag, L.; Reiher, M. Calculation of Ligand Dissociation Energies in Large Transition-Metal Complexes. *J. Chem. Theory Comput.* **2018**, *14*, 2456−2468.
(46) Momeni, M. R.; Brown, A. Why Do TD-DFT Excitation Energies of BODIPY/Aza-BODIPY Families Largely Deviate From Experiment? Answers From Electron Correlated and Multireference Methods. *J. Chem. Theory Comput.* **2015**, *11*, 2619−2632.
(47) Zhang, S.; Krakauer, H. Quantum Monte Carlo Method Using Phase-Free Random Walks With Slater Determinants. *Phys. Rev. Lett.* **2003**, *90*, 136401.
(48) Al-Saidi, W. A.; Zhang, S.; Krakauer, H. Auxiliary-Field Quantum Monte Carlo Calculations of Molecular Systems With a Gaussian Basis. *J. Chem. Phys.* **2006**, *124*, 224101.
(49) Shee, J.; Zhang, S.; Reichman, D. R.; Friesner, R. A. Chemical Transformations Approaching Chemical Accuracy via Correlated Sampling in Auxiliary-Field Quantum Monte Carlo. *J. Chem. Theory Comput.* **2017**, *13*, 2667−2680.
(50) Shee, J.; Arthur, E. J.; Zhang, S.; Reichman, D. R.; Friesner, R. A. Phaseless Auxiliary-Field Quantum Monte Carlo on Graphical Processing Units. *J. Chem. Theory Comput.* **2018**, *14*, 4109−4121.
(51) Luo, Y.-R. *Comprehensive Handbook of Chemical Bond Energies*; CRC press, 2007.
(52) Rodgers, M. T.; Armentrout, P. B. Cationic Noncovalent Interactions: Energetics and Periodic Trends. *Chem. Rev.* **2016**, *116*, 5642−5687.
(53) Hildenbrand, D. L. Low-Lying Electronic States and Revised Thermochemistry of TiCl, $TiCl_2$, and $TiCl_3$. *J. Phys. Chem. A* **2009**, *113*, 1472−1474.

https://dx.doi.org/10.1021/acs.jctc.0c00070
J. Chem. Theory Comput. 2020, 16, 3041−3054

(54) Coates, R. A.; Armentrout, P. B. Thermochemical Investigations of Hydrated Nickel Dication Complexes by Threshold Collision-Induced Dissociation and Theory. *J. Phys. Chem. A* **2017**, *121*, 3629−3646.
(55) Wells, J. R.; House, P. G.; Weitz, E. Interaction of H_2 and Prototypical Solvent Molecules with $Cr(CO)_5$ in the Gas Phase. *J. Phys. Chem.* **1994**, *98*, 8343−8351.
(56) Dalleska, N. F.; Honma, K.; Sunderlin, L. S.; Armentrout, P. B. Solvation of Transition Metal Ions by Water. Sequential Binding Energies of $M^+(H_2O)_x$ (x = 1−4) for M = Ti - Cu Determined by Collision-Induced Dissociation. *J. Am. Chem. Soc.* **1994**, *116*, 3519.
(57) Becke, A. D. Density-functional thermochemistry. III. The role of exact exchange. *J. Chem. Phys.* **1993**, *98*, 5648−5652.
(58) Vosko, S. H.; Wilk, L.; Nusair, M. Accurate Spin-Dependent Electron Liquid Correlation Energies for Local Spin Density Calculations: A Critical Analysis. *Can. J. Phys.* **1980**, *58*, 1200−1211.
(59) Lee, C.; Yang, W.; Parr, R. G. Development of the Colle-Salvetti Correlation-Energy Formula Into a Functional of the Electron Density. *Phys. Rev. B* **1988**, *37*, 785.
(60) Dunning, T. H. Gaussian Basis Sets for Use in Correlated Molecular Calculations. I. The Atoms Boron Through Neon and Hydrogen. *J. Chem. Phys.* **1989**, *90*, 1007.
(61) Woon, D. E.; Dunning, T. H. Gaussian Basis Sets for Use in Correlated Molecular Calculations. III. The Atoms Aluminum Through Argon. *J. Chem. Phys.* **1993**, *98*, 1358.
(62) de Jong, W. A.; Harrison, R. J.; Dixon, D. A. Parallel Douglas-Kroll Energy and Gradients in NWChem: Estimating Scalar Relativistic Effects Using Douglas-Kroll Contracted Basis Sets. *J. Chem. Phys.* **2001**, *114*, 48.
(63) Balabanov, N. B.; Peterson, K. A. Systematically convergent basis sets for transition metals. I. All-electron correlation consistent basis sets for the 3d elements Sc-Zn. *J. Chem. Phys.* **2005**, *123*, 064107.
(64) Neese, F. The ORCA Program System. *WIREs Comput. Mol. Sci.* **2012**, *2*, 73−78.
(65) Lewars, E. G. *Computational Chemistry. Introduction to the Theory and Applications of Molecular and Quantum Mechanics*; Springer, 2010; p 248.
(66) Riplinger, C.; Sandhoefer, B.; Hansen, A.; Neese, F. Natural Triple Excitations in Local coupled Cluster Calculations with Pair Natural Orbitals. *J. Chem. Phys.* **2013**, *139*, 134101.
(67) Flöser, B. M.; Guo, Y.; Riplinger, C.; Tuczek, F.; Neese, F. Detailed Pair Natural Orbital−based Coupled Cluster Studies of Spin Crossover Energetics. *J. Chem. Theory Comput.*. **2020**, *16*, 2224.
(68) Pantazis, D. A.; Chen, X.-Y.; Landis, C. R.; Neese, F. All-Electron Scalar Relativistic Basis Sets for Third-Row Transition Metal Atoms. *J. Chem. Theory Comput.* **2008**, *4*, 908−919.
(69) Sun, Q.; Berkelbach, T. C.; Blunt, N. S.; Booth, G. H.; Guo, S.; Li, Z.; Liu, J.; McClain, J. D.; Sayfutyarova, E. R.; Sharma, S.; Wouters, S.; Chan, G. K. PySCF: the Python-Based Simulations of Chemistry Framework. *WIREs Comput. Mol. Sci.* **2018**, *8*, e1340.
(70) Liu, W.; Peng, D. Exact Two-Component Hamiltonians Revisited. *J. Chem. Phys.* **2009**, *131*, 031104.
(71) Shee, J.; Arthur, E. J.; Zhang, S.; Reichman, D. R.; Friesner, R. A. Singlet-Triplet Energy Gaps of Organic Biradicals and Polyacenes with Auxiliary-Field Quantum Monte Carlo. *J. Chem. Theory Comput.* **2019**, *15*, 4924.
(72) Motta, M.; Zhang, S. Ab initio Computations of Molecular Systems by the Auxiliary-Field Quantum Monte Carlo Method. *WIREs Comput. Mol. Sci.* **2018**, *8*, e1364.
(73) DeYonker, N. J.; Peterson, K. A.; Steyl, G.; Wilson, A. K.; Cundari, T. R. Quantitative Computational Thermochemistry of Transition Metal Species. *J. Phys. Chem. A* **2007**, *111*, 11269−11277.
(74) Knizia, G. Intrinsic Atomic Orbitals: An Unbiased Bridge Between Quantum Theory and Chemical Concepts. *J. Chem. Theory Comput.* **2013**, *9*, 4834−4843.
(75) Sayfutyarova, E. R.; Sun, Q.; Chan, G. K.-L.; Knizia, G. Automated Construction of Molecular Active Spaces From Atomic Valence Orbitals. *J. Chem. Theory Comput.* **2017**, *13*, 4063−4078.
(76) Zhao, Y.; Truhlar, D. G. The M06 Suite of Density Functionals for Main Group Thermochemistry, Thermochemical Kinetics, Noncovalent Interactions, Excited States, and Transition Elements: Two New Functionals and Systematic Testing of Four M06-Class Functionals and 12 Other Functionals. *Theor. Chem. Acc.* **2008**, *120*, 215−241.
(77) Adamo, C.; Barone, V. Toward Reliable Density Functional Methods Without Adjustable Parameters: The PBE0 Model. *J. Chem. Phys.* **1999**, *110*, 6158−6170.
(78) Kozuch, S.; Martin, J. M. L. DSD-PBEP86: In Search of the Best Double-Hybrid DFT With Spin-Component Scaled MP2 and Dispersion Corrections. *Phys. Chem. Chem. Phys.* **2011**, *13*, 20104−20107.
(79) Kozuch, S.; Martin, J. M. Spin-Component-Scaled Double Hybrids: An Extensive Search for the Best Fifth-Rung Functionals Blending DFT and Perturbation Theory. *J. Comput. Chem.* **2013**, *34*, 2327−2344.
(80) Goerigk, L.; Hansen, A.; Bauer, C.; Ehrlich, S.; Najibi, A.; Grimme, S. A Look at the Density Functional Theory Zoo With the Advanced GMTKN55 Database for General Main Group Thermochemistry, Kinetics and Noncovalent Interactions. *Phys. Chem. Chem. Phys.* **2017**, *19*, 32184−32215.
(81) Santra, G.; Sylvetsky, N.; Martin, J. M. L. Minimally Empirical Double Hybrid Functionals Trained Against the GMTKN55 Database: revDSD-PBEP86-D4, revDOD-PBE-D4, and DOD-SCAN-D4. *J. Phys. Chem. A* **2019**, *24*, 5129.
(82) Walter, D.; Armentrout, P. B. Sequential Bond Dissociation Energies of $M^+(NH_3)_x$ (x = 1−4) for M = Ti−Cu. *J. Am. Chem. Soc.* **1998**, *120*, 3176.
(83) Holland, P. M.; Castleman, A. W. The thermochemical properties of gas-phase transition metal ion complexes. *J. Chem. Phys.* **1982**, *76*, 4195.
(84) Schultz, R. H.; Crellin, K. C.; Armentrout, P. B. Sequential Bond Energies of $Fe(CO)_x^+$ (x = 1−5): Systematic Effects on Collision-Induced Dissociation Measurements. *J. Am. Chem. Soc.* **1991**, *113*, 8590.
(85) Tjelta, B. L.; Armentrout, P. B. Gas-Phase Metal Ion Ligation: Collision-Induced Dissociation of $Fe(N_2)_x^+$ (x = 1−5) and $Fe(CH_2O)_x^+$ (x = 1−4). *J. Phys. Chem. A* **1997**, *101*, 2064.
(86) Distefano, G. Photoionization Study of $Fe(CO)_5$ and $Ni(CO)_4$. *J. Res. Natl. Bur. Stand., Sect. A* **1970**, *74A*, 233.
(87) Norwood, K.; Ali, A.; Flesch, G. D.; Ng, C. Y. A photoelectron-photoion coincidence study of iron pentacarbonyl. *J. Am. Chem. Soc.* **1990**, *112*, 7502.
(88) Khan, F. A.; Steele, D. L.; Armentrout, P. B. Ligand Effects in Organometallic Thermochemistry: The Sequential Bond Energies of $Ni(CO)_x^+$, $Ni(N_2)_x^+$ (x = 1−4) and $Ni(NO)_x^+$ (x = 1−3). *J. Phys. Chem.* **1995**, *99*, 7819.
(89) Coskun, D.; Jerome, S. V.; Friesner, R. A. Evaluation of the Performance of the B3LYP, PBE0, and M06 DFT Functionals, and DBLOC-Corrected Versions, in the Calculation of Redox Potentials and Spin Splittings for Transition Metal Containing Systems. *J. Chem. Theory Comput.* **2016**, *12*, 1121−1128.
(90) Harvey, J. N. On the Accuracy of Density Functional Theory in Transition Metal Chemistry. *Annu. Rep. Prog. Chem., Sect. C: Phys. Chem.* **2006**, *102*, 203−226.
(91) Grimme, S.; Hansen, A. A Practicable Real-Space Measure and Visualization of Static Electron-Correlation Effects. *Angew. Chem., Int. Ed.* **2015**, *54*, 12308−12313.
(92) Bauer, C. A.; Hansen, A.; Grimme, S. The Fractional Occupation Number Weighted Density as a Versatile Analysis Tool for Molecules With a Complicated Electronic Structure. *Chem.—Eur. J.* **2017**, *23*, 6150−6164.
(93) Lee, J.; Head-Gordon, M. Distinguishing Artificial and Essential Symmetry Breaking in a Single Determinant: Approach and Application to the C_{60}, C_{36}, and C_{20} fullerenes. *Phys. Chem. Chem. Phys.* **2019**, *21*, 4763−4778.
(94) Bauschlicher, C. W.; Siegbahn, P.; Pettersson, L. G. M. The Atomic States of Nickel. *Theor. Chim. Acta* **1988**, *74*, 479−491.

https://dx.doi.org/10.1021/acs.jctc.0c00070
J. Chem. Theory Comput. 2020, 16, 3041−3054

(95) Andersson, K.; Roos, B. O. Excitation Energies in the Nickel Atom Studied With the Complete Active Space SCF Method and Second-Order Perturbation Theory. *Chem. Phys. Lett.* **1992**, *191*, 507−514.
(96) Goerigk, L.; Grimme, S. Efficient and Accurate Double-Hybrid-Meta-GGA Density Functionals-Evaluation with the Extended GMTKN30 Database for General Main Group Thermochemistry, Kinetics, and Noncovalent Interactions. *J. Chem. Theory Comput.* **2010**, *7*, 291−309.
(97) Chan, B.; Radom, L. Accurate Quadruple−Zeta Basis-Set Approximation for Double-Hybrid Density Functional Theory With an Order of Magnitude Reduction in Computational Cost. *Theor. Chem. Acc.* **2014**, *133*, 1426−1429.
(98) Liakos, D. G.; Sparta, M.; Kesharwani, M. K.; Martin, J. M. L.; Neese, F. Exploring the Accuracy Limits of Local Pair Natural Orbital Coupled-Cluster Theory. *J. Chem. Theory Comput.* **2015**, *11*, 1525−1539.
(99) Ma, Q.; Werner, H.-J. Accurate Intermolecular Interaction Energies Using Explicitly Correlated Local Coupled Cluster Methods [PNO-LCCSD(T)-F12]. *J. Chem. Theory Comput.* **2019**, *15*, 1044−1052.
(100) Saitow, M.; Becker, U.; Riplinger, C.; Valeev, E. F.; Neese, F. A New Near-Linear Scaling, Efficient and Accurate, Open-Shell Domain-Based Local Pair Natural Orbital Coupled Cluster Singles and Doubles Theory. *J. Chem. Phys.* **2017**, *146*, 164105.
(101) Fang, Z.; Lee, Z.; Peterson, K. A.; Dixon, D. A. Use of Improved Orbitals for CCSD(T) Calculations for Predicting Heats of Formation of Group IV and Group VI Metal Oxide Monomers and Dimers and UCl_6. *J. Chem. Theory Comput.* **2016**, *12*, 3583−3592.
(102) Fang, Z.; Both, J.; Li, S.; Yue, S.; Aprà, E.; Keçeli, M.; Wagner, A. F.; Dixon, D. A. Benchmark Calculations of Energetic Properties of Groups 4 and 6 Transition Metal Oxide Nanoclusters Including Comparison to Density Functional Theory. *J. Chem. Theory Comput.* **2016**, *12*, 3689−3710.

https://dx.doi.org/10.1021/acs.jctc.0c00070
J. Chem. Theory Comput. 2020, 16, 3041−3054